Structure of the 1–36 N-Terminal Fragment of Human Phospholamban Phosphorylated at Ser-16 and Thr-17

Piero Pollesello* and Arto Annila†

*Orion Pharma, Cardiovascular Research, FIN-02101 Espoo, Finland; and †Department of Physical Sciences, University of Helsinki, FIN-00014 Helsinki, Finland

ABSTRACT The structure of a 36-amino-acid-long N-terminal fragment of human phospholamban phosphorylated at Ser-16 and Thr-17 and Cys-36→Ser mutated was determined from nuclear magnetic resonance data in aqueous solution containing 30% trifluoroethanol. The peptide assumes a conformation characterized by two α-helices connected by an irregular strand, which comprises the amino acids from Arg-13 to Pro-21. The proline is in a *trans* conformation. The two phosphate groups on Ser-16 and Thr-17 are shown to interact preferably with the side chains of Arg-14 and Arg-13, respectively. The helix comprising amino acids 22 to 35 is well determined (the rmsd for the backbone atoms, calculated for a family of 24 nuclear magnetic resonance structures is 0.69 ± 0.28 Å). The structures of phosphorylated and unphosphorylated phospholamban are compared, and the effect of the two phosphate groups on the relative spatial position of the two helices is examined. The packing parameters Ω (interhelical angle) and d (minimal interhelical distance) are calculated: in the case of the phosphorylated phospholamban, $\Omega = 100 \pm 35°$ and $d = 7.9 \pm 4.6$ Å, whereas for the unphosphorylated peptide the values are $\Omega = 80 \pm 20°$ and $d = 7.0 \pm 4.0$ Å. We conclude that 1) the phosphorylation does not affect the structure of the C terminus between residues 21 and 36 and 2) the phosphorylated phospholamban has more loose helical packing than the nonphosphorylated.

INTRODUCTION

Phospholamban (PLB) is a small protein (52 amino acids) that regulates the affinity of the cardiac sarcoplasmic reticulum Ca^{2+}-ATPase (SERCA2a) for calcium. The role of PLB in the regulation of the cardiac contraction has been defined by gene transfer (Kadambi et al., 1996) and knockout (Luo et al., 1994) technology in the mouse. PLB is present not only in cardiac myocytes but also in slow-twitch and smooth muscle. Recently, evidence was given that PLB is expressed also in aorta endothelial cells (Paul, 1998) in which it could play a role in the tissue relaxation (Sutliff et al., 1999).

PLB can be phosphorylated by both cAMP- (Karczewski et al., 1987) and Ca^{2+}/calmodulin-dependent phosphokinases (Iwasa et al., 1985). The phosphorylation/dephosphorylation of phospholamban removes and restores, respectively, its inhibitory activity on SERCA2a (Jackson and Colyer, 1996; Tada and Kadoma, 1989). It has been in fact shown that phospholamban, in its nonphosphorylated form, binds to SERCA2a and inhibits this pump by lowering its affinity for Ca^{2+}, whereas the phosphorylated form does not exert the inhibition (Toyofuku et al., 1993). PLB is phosphorylated at two sites, namely at Ser-16 for a cAMP-dependent phosphokinase and at Thr-17 for a Ca^{2+}/calmodulin-dependent phosphokinase. It was recently demonstrated that the phosphorylation at Ser-16 is a prerequisite for the phosphorylation at Thr-17 (Luo et al., 1998). Previous studies on a shorter fragment of PLB (1–20 amino acids) indicated that the phosphorylation leads to a local perturbation in the secondary structure (Mortishire-Smith et al., 1995) and to a weakened interaction with SERCA (Levine et al., 1999). Evidence was given for a specific interaction between Ser-16P and Arg-14 in a short PLB fragment (9–20 amino acids) (Quirk et al., 1996), whereas other authors, from MD simulation data, proposed that the guanidinium groups of both Arg-13 and Arg-14 have the potential to interact with the phosphoryl group of Ser-16P (Mortishire-Smith et al., 1995, 1998). Recently, the structure of a 36-amino-acid-long N-terminal fragment of PLB (PLB36) in aqueous solution containing 30% trifluoroethanol (TFE) was determined by nuclear magnetic resonance (NMR) (Pollesello et al., 1999), and PLB was shown to assume a conformation in which two α-helices are connected by a less structured turn centered at residues Glu-19-Pro-21 (near the PLB phosphorylation sites). In the present study the structure of the 36-residue N-terminal fragment of PLB phosphorylated at both Ser-16 and Thr-17 is determined. The structures obtained for the phosphorylated and unphosphorylated PLB1–36 under the same experimental conditions are compared, and the effect of the phosphorylation is discussed.

MATERIALS AND METHODS

Synthesis of the doubly phosphorylated phospholamban fragment

The 36-amino acid PLB peptide phosphorylated at Ser-16 and Thr-17 and with a mutation at the carboxy terminus (Cys-36→Ser) was synthesized at MedProbe AS (Norway). The Cys-36→Ser mutation at the C terminus was introduced to prevent dimerization, rather then using DTT_{d10}, otherwise required for the protection of the Cys SH group. The peptide was purified

Submitted December 4, 2001, and accepted for publication March 27, 2002.

Address reprint requests to Piero Pollesello, Orion Pharma, Cardiovascular Research, P.O. Box 65, FIN-02101 Espoo, Finland. Tel.: 358-50-429-4191; Fax: 358-10-429-2924; E-mail: piero.pollesello@orionpharma.com.

0006-3495/02/07/484/07 $2.00

by reverse phase high-pressure liquid chromatography using a C-18, 5 μm, 250 $\times$ 4.6-mm column. A linear gradient of acetonitrile and 0.075% trifluoroacetic acid (TFA) (20%–50% in 30 min) in 0.1% TFA was used for elution. The purified peptide was further characterized by MALDI-TOF mass spectrometry in reflector mode with a BIFLEX mass spectrometer using a 337-nm nitrogen laser for the ionization of the sample. The sample was applied in a solution containing 30% acetonitrile/0.1% TFA together with a droplet of sinapinic acid matrix for mass spectrometry analysis. The total amount of purified peptide was 10 mg, and the purity of the peptide was 96% according to mass spectrometry and high-pressure liquid chromatography.

NMR spectra

^{1}H- and ^{31}P-NMR spectra were acquired at 600 and 242 MHz, respectively, on a Varian UNITY600 NMR spectrometer. One-dimensional and two-dimensional NMR spectra were obtained for a 3-mM solution of the 36-amino acids fragment of phospholamban phosphorylated on Ser-16 and Thr-17 (C36S mutated) in the solvent mixture $H_2O/D_2O/d_3$-TFE (perdeuterated trifluoroethanol) (63:7:30). The pH was adjusted to 3.05 $\pm$ 0.05 (uncorrected for deuterium isotope effects) with microliter amounts of NaOD. Correlation spectroscopy (COSY), total correlation spectroscopy (30–90 ms), and nuclear Overhauser-effect spectroscopy (NOESY) (40–200 ms) spectra were recorded at 17°C and 27°C by the States-time proportional phase incrementation method (Marion et al., 1989), using a spectral width of 8.5 ppm. The two-dimensional data were weighted and Fourier transformed to 2 k $\times$ 1 k real point matrices. The transmitter presaturated (2.0 s) residual solvent line was reduced by deconvolution, and NOESY data was taken with the Watergate sequence (Piotto et al., 1992). The spectra were referenced to the residual solvent signal (4.75 ppm at 27°C, -0.01 ppm/°C). A series of 10 one-dimensional spectra was acquired at different temperatures from 2°C to 47°C (data not shown) to investigate the temperature dependence of the chemical shifts of the backbone NH protons.

Assignment of the NMR spectra

The spectra of di-P-(C36S)PLB36 (36-amino acid N-terminal fragment of human phospholamban Cys-36$\rightarrow$Ser mutated and phosphorylated at Ser-16 and Thr-17) display good chemical shift dispersion. The complete spin-system and sequential assignments were obtained according to Wüthrich (1986) by use of COSY, total correlation spectroscopy, and NOESY spectra acquired at 17°C and 27°C. Differences in the temperature dependence of the amido proton chemical shifts were sufficient to unravel resonance overlap. Stereospecific assignments for the methylene protons were deduced from coupling constants $J_{H\alpha H\beta}$ measured from the COSY spectra and from intraresidual nuclear Overhauser enhancement (NOE)-cross-peak intensities.

Structure generation and refinement

A series of NOESY spectra was acquired at 17°C with four different mixing times (50, 80, 120, 170 ms). The integrated cross-peak intensities (I) were used in a NOESY-build-up analysis. Distance restraints were extracted from the initial slope of a second-order polynomial fitted to integrated cross-peak volumes of the NOE-series with the initial condition $I(\tau_m = 0) = 0$. Some of the intramethylene and sequential NOEs served for the calibration. When a distance could not be extracted from the build-up curve, owing to a partial (>10%) overlap, a poor signal-to-noise ratio or disturbances, it was only required that the distance was at most 6.0 Å. The upper bounds were extended by 1.0 Å for each pseudo atom. The distances were initially classified as short, medium, and long to provide restrains for the generation of the first set of structures. The restraint data were supplemented with distance restraints derived from the 200-ms NOE-spectrum acquired at 17°C. During the refinement the distances from the NOESY-build-up analysis were given a $-40\%/+10\%$ uncertainty and from the 200-ms NOE-spectrum a $-50\%/+20\%$ uncertainty.

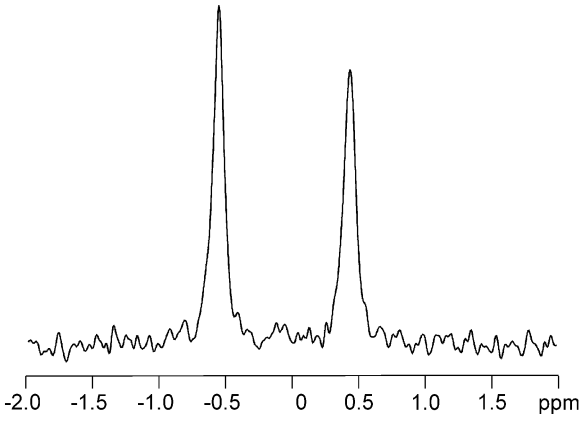

FIGURE 1 ^{31}P-NMR spectrum acquired at 242 MHz for a sample of 3 mM di-P-(C36S)PLB36 in $H_2O/D_2O/d_3$-TFE (63:7:30). The pH was adjusted to 3.05 $\pm$ 0.05 (uncorrected for deuterium isotope effects). The assignments are 0.56 ppm for phosphoserine and -0.43 ppm for phosphothreonine. The scale (in ppm) is referenced with respect to CTP.

Coupling constants (J) were measured by the J-doubling method (McIntyre and Freeman, 1992) from the fine structures of COSY cross-peaks. Dihedral angles ϕ and χ characterized by intermediate J values were not constrained, but small and large $J_{NH\alpha}$ and $J_{H\alpha H\beta}$ were related to staggered conformers ($\pm$30°) on the basis of Karplus functions and intraresidual NOEs. The H-H distance and dihedral angle restraints were calculated with the software FELIX (MSI). Finally, the data were imported in the software InsightII (MSI) to create, evaluate and refine a family of structures, and, eventually, to back calculate simulated NOESY spectra for comparison.

Structures were generated by distance geometry (DGII) followed by simulated annealing (force field cvff). A set of 50 structures was computed. The structures with least restraint violations were used to back calculate NOE matrices. Based on the comparison of the back-calculated and experimental NOE spectra it became possible to unambiguously identify a few more NOEs and impose corresponding distance restraints. Also the ψ dihedral angles in the α-helical segments were constrained ($\pm$60°) provided that an Hα-chemical shift departed from the corresponding random coil value by more than -0.2 ppm. A new set of structures was subsequently calculated. In total there were 530 distance and 27 dihedral angle restraints excluding those that were defined more accurately by the covalent structure alone. These redundant NOE-derived restraints were consistent with the covalently imposed limits obtained from the sequential tetragonal bound smoothing, which indicated that the calibration of distances was correct. The restraint violations of the final accepted family of structures were below 0.1 Å. Finally, to consider the role of Coulombic interaction between the phosphorous of Ser-16 and Thr-17 with Arg-9, Arg-13, and Arg-14 the final family of structures were subjected to a minimization in the presence of charges and NMR-based restraints. The distance dependent dielectric constant was given value of 1.4 F $\times$ m^{-1}.

RESULTS AND DISCUSSION

Preparation of the sample

Solubility tests were performed to assess which conditions (TFE concentration, temperature, pH values) were suitable

TABLE 1 ^{1}H-NMR assignment of 36-amino acid fragment of phospholamban phosphorylated on Ser-16 and Thr-17 (C36 → S mutated) in the solvent mixture $H_2O/D_2O/d_3$-TFE (63:7:30)

				HB		HG			HD		HE	
Amino acid	#	HN	HA	HB1/ HB*	HB2	HG1/HG*/ HG1*/HG11	HG2/ HG12	HG2*	HD1/HD*/ HD1*/HD21	HD2/ HD2*/HD22	HE*/ HE21	HE22
MET	1		4.152	2.103		2.569						
GLU	2	8.760	4.534	2.232	1.962	2.477						
LYS	3	8.639	4.200	1.838	1.510	1.410			1.684		2.915	
VAL	4	8.183	3.921	2.077		0.970		0.887				
GLN	5	8.035	4.129	2.083	2.021	2.276					7.425	6.784
TYR	6	7.882	4.360	3.088	3.002				7.036		6.762	
LEU	7	8.218	4.156	1.749	1.698	1.567			0.884	0.876		
THR	8	7.828	4.159	4.269			1.219					
ARG	9	7.997	4.190	1.859		1.662			3.138		7.206	
SER	10	8.018	4.289	3.871	3.779							
ALA	11	7.945	4.255	1.421								
ILE	12	7.734	4.048	1.856		1.535	1.164	0.807	0.870			
ARG	13	8.031	4.401	1.859	1.755	1.679	1.609		3.182		7.381	
ARG	14	8.704	4.413	2.020	1.879	1.665			3.180		7.500	
ALA	15	8.492	4.178	1.439								
SER	16	8.531	4.442	4.221	4.172							
THR	17	7.859	4.526	4.795				1.289				
ILE	18	7.757	4.056	1.861			1.186	0.813	0.905			
GLU	19	8.217	4.392	2.127		2.453						
MET	20	7.965	4.682	2.050		2.532						
PRO	21		4.482	2.493	1.956	2.063			3.930	3.602		
GLN	22	8.921	4.002	2.074		2.440					7.458	6.763
GLN	23	8.888	4.092	2.091		2.453					7.485	6.819
ALA	24	7.421	4.147	1.468								
ARG	25	7.872	3.930	1.867		1.682	1.583		3.189		7.295	
GLN	26	8.114	4.040	2.124		2.462	2.363				7.387	6.740
LYS	27	7.660	4.063	1.948	1.446	1.676	1.593				2.944	
LEU	28	8.117	4.015	1.769	1.704	1.518			0.857	0.812		
GLN	29	8.189	4.012		2.103	2.484	2.360				7.192	6.697
ASN	30	7.915	4.488	2.892	2.801				7.495	6.836		
LEU	31	7.905	4.124	1.723	1.625	1.516			0.851	0.791		
PHE	32	8.117	4.396	3.213	3.079				7.176		7.228	
ILE	33	8.025	3.918			1.628	1.233	0.849	0.871			
ASN	34	7.893	4.577	2.620	2.533				7.282	6.765		
PHE	35	7.991	4.710	3.269	3.021				7.269		7.212	
SER	36	7.777	4.398	3.917	3.833							

The pH was adjusted to 3.05 ± 0.05 (uncorrected for deuterium isotope effects).

for a stable aqueous NMR sample containing millimolar concentrations of di-P-(C36S)PLB36. Among some possible solutions, it was preferential to prepare a 3-mM solution of the 36-amino acids fragment of phosphorylated phospholamban in the solvent mixture $H_2O/D_2O/d_3$-TFE (63:7:30) at pH 3.05 ± 0.05 and to study this sample at 27°C. This choice was also dictated by the fact those conditions were the same at which the unphosphorylated PLB1–36 was soluble, and it was thus possible to compare the structures obtained for phosphorylated and unphosphorylated PLB1–36 in the same solution. It should be pointed out that the phosphate groups maintain one net charge at the pH value selected for the experiment. In fact, for phosphoserine and phosphothreonine peptides, the pK_{a1} of the phosphoryl group lies below 2, whereas the pK_{a2} is at 5.9 (Hoffmann et al., 1994). The presence of TFE, also needed for the solubility, could be important also to mimic the transmembrane environment of part of the peptide. A ^{31}P-NMR spectrum was acquired (Fig. 1) and shows two well-resolved peaks that could be assigned to phosphoserine (+0.56 ppm) and phosphothreonine (−0.43 ppm).

Assignment

The complete spin-system and sequential assignments are listed in Table 1. More than 600 NOEs were assigned, and all of the 34 possible intra-NH-C_αH correlations were observed in the finger-print region. The secondary shift ($\Delta\delta$) of αCH (defined as the difference between the chemical shift observed for di-P-(C36S)PLB36 in aqueous solution at pH 3.05 with 30% TFE and the random

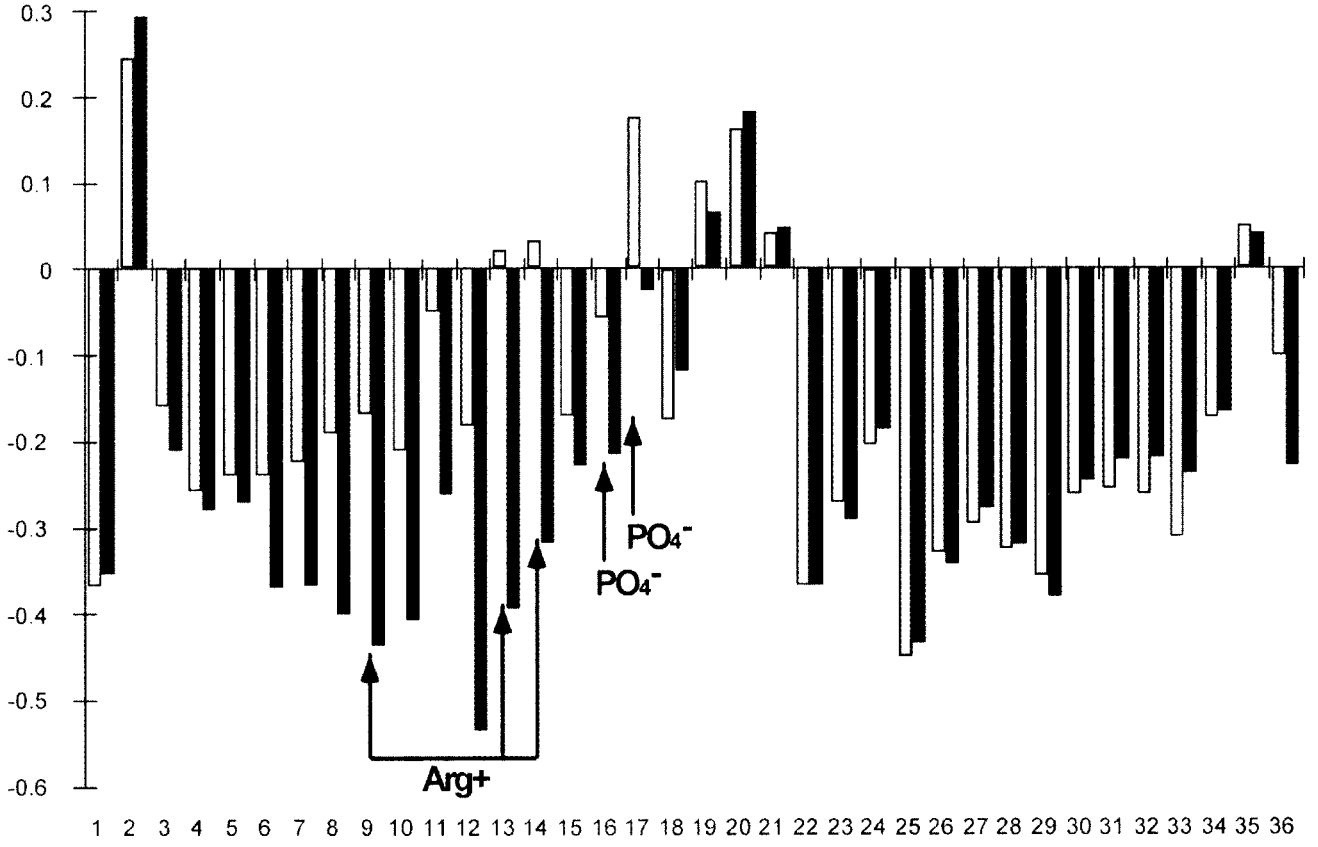

FIGURE 2 The secondary shift ($\Delta\delta$) of the αCH (defined as the difference between the chemical shift of the αCH of each amino acid observed in the peptides with the correspondent value observed in a random coil conformation) is plotted for every residue in sequence of di-P-(C36S)PLB36 and PLB36 in water solution at pH 3.05 with 30% TFE. Negative (upfield) $\Delta\delta$ values are associated with α-helical secondary structure and positive (downfield) $\Delta\delta$ values with β-structure (Wishart et al., 1992). The values indicate that the residues in the region from Arg-9 to Ile-18 are much less structured in the phosphorylated peptide than in the nonphosphorylated.

coil chemical shift for each residue) is shown in Fig. 2. Negative (upfield) $\Delta\delta$ values are related to α-helical secondary structure (Wishart et al., 1992). In the same figures, for comparison, the secondary shift of αCH of the nonphosphorylated PLB36, acquired at the same conditions, are shown (Pollesello et al., 1999). The region from Arg-9 to Ile-18 appears much less structured in di-P-(C36S)PLB36 than in the unphosphorylated peptide. Such data are in agreement with the results of Quirk et al. (1996) obtained for shorter PLB peptides in phosphorylated and unphosphorylated form. The one-dimensional NMR spectra of 3 mM di-P-(C36S)PLB36 in 63% H_2O/7% D_2O/30% d_3-TFE, pH 3.05 $\pm$ 0.05, were acquired at different temperatures, namely from 0°C to 40°C in 5°C steps (data not shown). The temperature-dependent shift of a number of the backbone NH protons do not follow the temperature-dependent shift of the water (-10 ppb/°C), thus indicating the presence of several H-bonds. When compared with the same spectra acquired for the unphosphorylated PLB (Pollesello et al., 1999) it can be noticed that the overall dispersion of the NH peaks in the fingerprint region ($9 > \delta > 7$ ppm) is similar for di-P-(C36S)PLB36 and PLB36.

TABLE 2 Characteristics of the structures

Parameters	Number of NOE-restraints
Short range	299
Medium range ($i + 4$)	229
Long range ($>i + 4$)	2
Total	530

Parameters	rmsd (Å) for backbone atoms	rmsd (Å) for all atoms
For region 1–15	1.66 $\pm$ 0.78	3.38 $\pm$ 0.92
For region 1–17	2.14 $\pm$ 0.68	3.67 $\pm$ 0.89
For region 22–36	0.53 $\pm$ 0.16	2.02 $\pm$ 0.29

Data were computed from a family of 24 structures with no violations >0.1Å. Short range are restraints within the same residue; medium and long range are restraints within residues with sequence separation $\leq$4 and $\geq$4, respectively. On the average there were 14.4 nontrivial NOE-derived restraints per residue.

Number of Φ and Ψ angles in core or allowed in the Ramachandran plot: 94%.

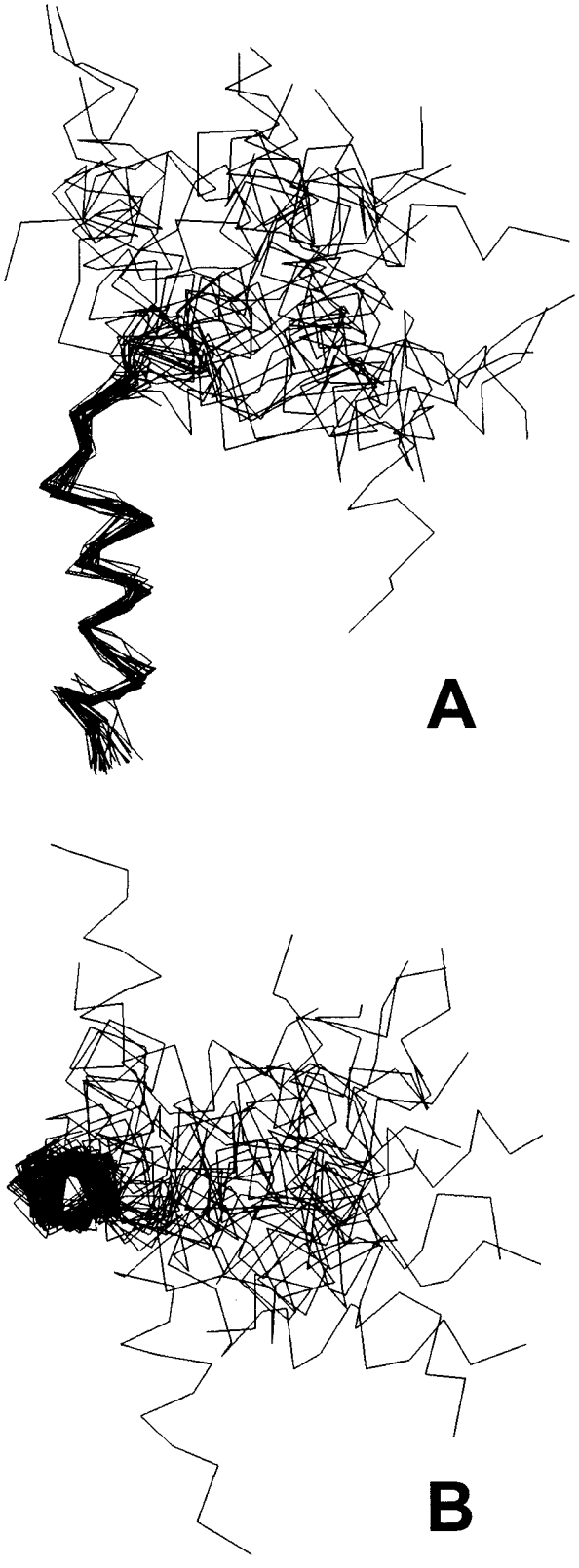

FIGURE 3 Structures of di-P-(C36S)PLB36 deduced from NMR data. Twenty-four structures with no violations >0.1 Å are superimposed on the Cα of the residues 22 to 35 in the C-terminal helix. The root mean square deviation for the backbone atoms from residue 22 to 35, calculated for this family of structures is 0.69 ± 0.28 Å. The N-terminal helices of the 24 structures appear dispersed in a cone with an opening of ~80°. The interhelix angle is 110 ± 40° (n = 26). (*A* and *B*) Orthogonal views of the structure family

Structure of di-P-(C36S)PLB36

The structure of di-P-(C36S)PLB36 was determined from 530 distance and 27 dihedral restraints excluding those that were defined more accurately by the covalent structure alone (Table 2). Twenty-four structures of di-P-(C36S)PLB36 deduced from NMR data with no violations >0.1 Å are shown in Fig. 3 after being superimposed on the Cα of the residues 22–35. In all of the structures, both the C-terminal fragment (from amino acids 22–35) and the N terminus (from amino acids 2–12) are α-helices. When superimposing the 24 NMR structures on the C-terminal helix, the N-terminal helix appears dispersed in a cone with an opening angle of ~80°. To compare the structures of the phosphorylated and nonphoaphorylated PLB peptides was convenient to compute the so called "packing parameters" (defined for α-helix dimers by Chothia et al. (1981) for the two sets of structures and compare the average values of the crossing angle Ω (defined as the torsion angle between the axes of the two helices when projected on a contact plane) and the distance of closest contact d in the two sets. According to the definition, for Ω = 0° the two helices are perfectly parallel and orthogonal for Ω = 90°. When the axes of the two helices are on the same plane, d = 0. In the case of di-P-(C36S)PLB36, Ω = 100 ± 35° and d = 7.9 ± 4.6 Å, when the average and standard deviation values were calculated over 24 structures with no violations >0.1 Å. The values of Ω and d for the unphosphorylated PLB36 were 80 ± 20° and 7.0 ± 4.0 Å, respectively, when calculated for the family of 18 structures with no violations >0.2 Å shown in our previous paper (Pollesello et al., 1999). Therefore neither in the nonphosphorylated nor in the phosphorylated PLB structures the two α-helices are closely packed. However, the standard deviation of the Ω value obtained for the phosphorylated peptide is larger than for the unphosphorylated peptide, indicating even more loose packing.

We attribute the very loose packing of the phosphorylated peptide to the phosphorylated amino acids that disrupt the N-terminal helix adjacent to the turn connecting to the C-terminal helix (Fig. 2). Whereas in the nonphosphorylated PLB the region from Arg-13 to Thr-17 is an α-helix and only the short region from Ile-18 to Pro-21 is a less structured turn (Pollesello et al., 1999).

It appears that the two helices are further apart from each other in the phosphorylated peptide than in the nonphosphorylated form. However, structural integrity in the phosphorylated region may still be present due to ionic bridges between the phosphate groups of the two phosphorylated

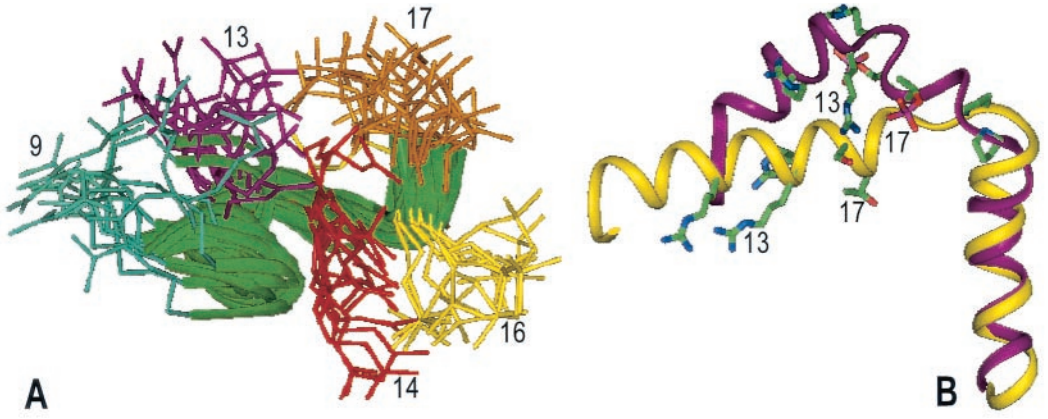

FIGURE 4 Structures of di-P-(C36S)PLB36 deduced from NMR data. (*A*) Backbone ribbons from Arg-9 to Thr-17 and the side chains of amino acids Arg-9 (*cyan*), Arg-13 (*magenta*), Arg-14 (*red*), Ser-16 (*yellow*), and Thr-17 (*gold*) of the structures of di-P-(C36S)PLB36 are shown after superimposing the backbones. The proximity of the positively charged side chain of Arg-13 with the negatively charged phosphate group of Thr-17 can be seen, as well as the proximity of Arg-14 with Ser-16. (*B*) Structure of di-P-(C36S)PLB36 with the fewest NOE violation (*magenta*) and the structure of PLB36 with the fewest NME violation (*yellow*) described elsewhere (Pollesello et al., 1999) are shown after being superimposed in their C-terminal α-helices (from amino acids 22–35). The side chains of amino acids Arg-9, Arg-13, Arg-14, Ser-16, Thr-17, and Pro-21 are shown on the backbone ribbons of the two peptides.

amino acids (Ser-16 and Thr-17) and two arginines (Arg-13 and Arg-14).

When minimizing the structures in the presence of Coulumbic interactions, we found favorable interactions between the side chain groups. In the majority of the structures of the family, in fact, the distance from the carbon CZ of Arg-13 to the phosphorus atom of Thr-17 is between 3.85 and 5.50 Å, and the distance from the carbon CZ of Arg-14 to the phosphorus atom of Ser-16 is between 4.25 and 6.00 Å (Fig. 4 *A*). In a few structures of the family, also Arg-25 comes close to the phosphate group of Ser-16, whereas Arg-9 is never close to either phosphate groups. A comparison of the structure of di-P-(C36S)PLB36 and PLB36 is shown in Fig. 4 *B*, where two representative structures are superimposed on the Cα of the residues 22–35. It can be noticed that the interaction between the phosphate groups and the arginine polar heads in di-P-(C36S)PLB36 create a second bend (the first being located on the proline residue) with the result that the distance between the two α-helices in di-P-(C36S)PLB36 is bigger than in PLB36. The structure shown in Fig. 4 is consistent with the structural data on the direct effects of phosphorylation on the preferred backbone conformation of peptides described by Tholey et al. (1999).

A molecular model of the transmembrane domain of phospholamban was proposed, in which a symmetric homopentamer composed of a left-handed coiled coil of α-helices (Simmerman et al., 1996) is stabilized by a leucine-isoleucine zipper. In a separate publication (Pollesello et al., 1999), the structure PLB36 was resolved by NMR and connected to the transmembrane pentamer model proposed previously. In this way a model of the whole phospholamban in its pentameric form was generated in which the inner side of the cytoplasmic domain of the pentamer (where the helices face one another) was lined by polar residues (Gln-23, Gln-26, and Asn-30), whereas the positively charged Arg-25 and Lys-27 side chains were on the outer side.

Because the present data show that the phosphorylation of PLB36 occurs without any modification of the structure in the fragment 21–36, which remains as a well-characterized α-helix, it is possible to use the same docking method described previously and build a model of the phosphorylated PLB pentamer. Molecular modeling was performed to evaluate if the interaction between the phosphate groups of one monomer and the Arg-25 or Lys-27 of the neighbor monomers in the pentamer is possible. The data (not shown) did not confirm this hypothesis because in all the structures analyzed none of the phosphate groups on the N terminus was close to any of the positively charged groups of the C terminus of the neighbor monomers.

Indeed, a role of the phosphorylation in the stabilization of the PLB pentamer structure was proposed by Cornea et al. (1997). The authors performed electron paramagnetic resonance experiments on lipid reconstituted recombinant PLB, showed a phosphorylation-dependent increase in the degree of oligomerization, but concluded that this effect was due simply to a reduced electrostatic repulsion among the phosphorylated PLB monomers. This explanation, not based on any specific interdomain electrostatic interaction, is consistent with our data.

Recently, the structure of a point mutated (Cys-41→Phe) monomeric PLB was resolved by NMR in a mixture of organic solvents ($CHCl_3$/MeOH) (Lamberth et al., 2000). The family of structures shown in that paper was consistent with the data obtained for PLB36 in water/TFE (Pollesello et al., 1999). It would be of interest to compare the structure

of the di-phosphorylated PLB in the different two solvent systems to understand if the structural changes induced by the two phosphate groups are 1) independent of the environment and 2) maintained also in the whole length PLB.

REFERENCES

Chothia, C., M. Levitt, and D. Richardson. 1981. Helix to helix packing in proteins. *J. Mol. Biol.* 145:215–250.

Cornea, R. L., L. R. Jones, J. M. Autry, and D. D. Thomas. 1997. Mutation and phosphorylation change the oligomeric structure of phospholamban in lipid bilayers. *Biochemistry.* 36:2960–2967.

Hoffmann, R., I. Reichert, W. Wachs, M. Zeppezauer, and H.-R. Kalbitzer. 1994. ^{1}H and ^{31}P NMR spectroscopy of phosphorylated model peptides. *Int. J. Pept. Protein Res.* 44:193–198.

Iwasa, T., N. Inoue, and E. Miyamoto. 1985. Identification of a calmodulin-dependent protein kinase in the cardiac cytosol, which phosphorylates phospholamban in the sarcoplasmic reticulum. *J. Biochem.* 98: 577–580.

Jackson, W. A., and J. Colyer. 1996. Translation of Ser^{16} and Thr^{17} phosphorylation of phospholamban into Ca^{2+}-pump stimulation. *Biochem. J.* 316:201–207.

Kadambi, V. J., S. Ponniah, J. M. Harrer, B. D. Hoit, G. W. Dorn, R. A. Walsh, and E. G. Kranias. 1996. Cardiac-specific overexpression of phospholamban alters calcium kinetics and resultant cardiomyocyte mechanics in transgenic mice. *J. Clin. Invest.* 97:533–539.

Karczewski, P., S. Bartel, H. Haase, and E. G. Krause. 1987. Isoproterenol induces both cAMP- and calcium-dependent phosphorylation of phospholamban in canine heart in vivo. *Biomed. Biochim. Acta.* 46: S433–S439.

Lamberth, S., H. Schmid, M. Muenchbach, T. Vorherr, J. Krebs, E. Carafoli, and C. Griesinger. 2000. NMR solution structure of phospholamban. *Helv. Chim. Acta.* 83:2141–2152.

Levine, B. A., V. B. Patchell, P. Sharma, Y. Gao, D. J. Bigelow, Q. Yao, S. Goh, J. Colyer, G. A. Drago, and S. V. Perry. 1999. Sites on the cytoplasmic region of phospholamban involved in interaction with the calcium-activated ATPase of the sarcoplasmic reticulum. *Eur. J. Biochem.* 264:905–913.

Luo, W., G. Chu, Y. Sato, Z. Zhou, V. J. Kadambi, and E. G. Kranias. 1998. Transgenic approaches to define the functional role of dual site phospholamban phosphorylation. *J. Biol. Chem.* 273:4734–4739.

Luo, W., I. L. Grupp, J. Harrer, S. Ponniah, G. Grupp, J. J. Duffy, T. Doetschman, and E. G. Kranias. 1994. Targeted ablation of the phospholamban gene is associated with markedly enhanced myocardial contractility and loss of β-agonist stimulation. *Circ. Res.* 75:401–409.

Marion, D., M. Ikura, R. Tschudin, and A. Bax. 1989. Rapid recording of 2D NMR spectra without phase cycling: application to the study of hydrogen exchange in proteins. *J. Magn. Reson.* 85:393–399.

McIntyre, L., and R. Freeman. 1992. Accurate measurements of coupling constants by *J* doubling. *J. Magn. Reson.* 96:425–431.

Mortishire-Smith, R. J., H. Broughton, V. M. Garsky, E. J. Mayer, and R. J. J. Johnson. 1998. Structural studies on phospholamban and implications for regulation of the Ca^{2+}-ATPase. *Ann. N.Y. Acad. Sci.* 853: 63–78.

Mortishire-Smith, R. J., S. M. Pitzenberger, C. J. Burke, C. R. Middaugh, V. M. Garsky, and R. G. Johnson. 1995. Solution structure of the cytoplasmic domain of phospholamban: phosphorylation leads to a local perturbation in secondary structure. *Biochemistry.* 34:7603–7613.

Paul, R. J. 1998. The role of phospholamban and SERCA-3 in regulation of smooth muscle-endothelial cell signalling mechanisms: evidence from gene-ablated mice. *Acta Physiol. Scand.* 164:589–597.

Piotto, M., V. Saudek, and V. Sklenar. 1992. Gradient-tailored excitation for single-quantum NMR spectroscopy of acqueous solutions. *J. Biomol. N.M.R.* 2:661–665.

Pollesello, P., A. Annila, and M. Ovaska. 1999. Structure of the 1–36 amino-terminal fragment of human phospholamban by nuclear magnetic resonance and modeling of the phospholamban pentamer. *Biophys. J.* 76:1784–1795.

Quirk, P., V. Patchell, J. Colyer, G. Drago, and Y. Gao. 1996. Conformational effects of serine phosphorylation in phospholamban peptides. *Eur. J. Biochem.* 236:85–91.

Simmerman, H. K. B., Y. M. Kobayashi, J. M. Autry, and L. R. Jones. 1996. A leucine zipper stabilizes the pentameric membrane domain of phospholamban and forms a coiled-coil pore structure. *J. Biol. Chem.* 271:5941–5946.

Sutliff, R. L., J. B. Hoying, V. J. Kadambi, E. G. Kranias, and R. J. Paul. 1999. Phospholamban is present in endothelial cells and modulates endothelium-dependent relaxation evidence from phospholamban gene-ablated mice. *Circ. Res.* 84:360–364.

Tada, M., and M. Kadoma. 1989. Regulation of the Ca^{2+} pump ATPase by cAMP-dependent phosphorylation of phospholamban. *Bioessays.* 10: 157–163.

Tholey, A., A. Lindemann, V. Kinzel, and J. Reed. 1999. Direct effects of phosphorylation on the preferred backbone conformation of peptides: a nuclear magnetic resonance study. *Biophys. J.* 76:76–87.

Toyofuku, T., K. Kurzydlowski, M. Tada, and D. H. MacLennan. 1993. Identification of regions in the Ca^{2+}-ATPase of sarcoplasmic reticulum that affect functional association with phospholamban. *J. Biol. Chem.* 268:2809–2815.

Wishart, D. S., B. D. Sykes, and F. M. Richards. 1992. The chemical shift index: a fast and simple method for the assignment of protein secondary structure through NMR spectroscopy. *Biochemistry.* 31:1647–1651.

Wüthrich, K. 1986. NMR of Proteins and Nucleic Acids. John Wiley and Sons, Inc., New York.